Structural Engineering and Mechanics, Vol. 33, No. 4 (2009) 391-406
DOI: http://dx.doi.org/10.12989/sem.2009.33.4.391

Dynamics of multilayered viscoelastic beams

H. Roy†

Department of Mechanical Engineering
National Institute of Technology, Rourkela-769008, Orissa, India

J.K. Dutt‡

Department of Mechanical Engineering
Indian Institute of Technology, Delhi, Hauz Khas, 110016, New Delhi, India

P.K. Datta‡†

Department of Aerospace Engineering
Indian Institute of Technology, Kharagpur-721302, West Bengal, India

(Received November 7, 2007, Accepted May 12, 2009)

Abstract. Viscoelastic materials store as well as dissipate energy to the thermal domain under deformation. Two efficient modelling techniques reported in literature use coupled (thermo-mechanical) ATF (Augmenting Thermodynamic Fields) displacements and ADF (Anelastic Displacement Fields) displacements, to represent the constitutive relationship in time domain by using certain viscoelastic parameters. Viscoelastic parameters are first extracted from the storage modulus and loss factor normally reported in hand books with the help of Genetic Algorithm and then constitutive relationships are used to obtain the equations of motion of the continuum after discretizing it with finite beam elements. The equations of motion are solved to get the frequency response function and modal damping ratio. The process may be applied to study the dynamic behaviour of composite beams and rotors comprising of several viscoelastic layers. Dynamic behaviour of a composite beam, formed by concentric layers of steel and aluminium is studied as an example.

Keywords: viscoelastic beam; augmenting thermodynamic field; anelastic displacement field; viscoelastic model parameters; modal damping ratio; composite beam.

1. Introduction

A viscoelastic material stores energy and dissipates it in the thermal domain when subjected to dynamic loading and most interestingly the storage and loss of energy depends upon the frequency of excitation. To find a time domain model to represent the behaviour of viscoelastic solids found

† Lecturer, Ph.D., Corresponding author, E-mail: hroy77@rediffmail.com
‡ Associate Professor, E-mail: jkrdutt@yahoo.co.in
‡† Professor, E-mail: pkdatta@aero.iitkgp.ernet.in

interest of many researchers. Bagley and Torvik (1983, 1985) represented frequency dependent behaviour of viscoelastic solids by using four-model parameters and differential operators of fractional order. The time-domain model with ordinary integer differential operators was developed by Golla and Hughes (1985), who incorporated the hereditary integral form of the viscoelastic constitutive law in a finite element model. The finite-element equations are derived in the Laplace domain through the Ritz technique. McTavish and Hughes (1992, 1993) extended the Golla-Hughes model and formulated the GHM (Golla-Hughes-McTavish) model for linear viscoelastic structures. In this formulation, the material modulus is modelled as a collection of mini-oscillators. Lesieutre (1989) developed another time-domain model, using 'Augmenting Thermodynamic Fields (ATF)' approach to model frequency-dependent material-damping of linear viscoelastic structures in a finite element context. The procedure introduces a thermal coordinate to take into account the dissipation. Lesieutre and Mingori (1990) and later Lesieutre (1992) developed a one-dimensional formulation of the ATF model. In a recent paper, Roy *et al.* (2008) used the ATF approach to model a viscoelastic continuum of a rotor shaft, to obtain the equations of motion and studied the dynamic behaviour in terms of stability limit speed and unbalance response. The 'Anelastic Displacement Field' ADF, (Lesieutre and Bianchini (1995), Lesieutre *et al.* (1996)) approach was developed to extend the ATF method to three-dimensional states. In ADF approach, the displacement field was composed of an elastic component and an anelastic component, where the anelastic field is introduced to take in to account the dissipation. All the approaches, ATF, ADF and GHM thus employ additional co-ordinates to model damping more accurately. Whereas the 'dissipation co-ordinate' of GHM is internal to individual elements, it is continuous for ATF and ADF approaches from element to element. For this advantage ATF and ADF approaches are used in this work to represent the viscoelastic material behaviour.

Viscoelastic parameters used in these approaches are determined initially from the storage modulus and loss factor reported by Lazan (1968). For this a Genetic Algorithm based approach is adopted to minimize the error between the hysteresis loops predicted by ATF, ADF approaches each and the same predicted by the complex modulus, for a viscoelastic solid bar under sinusoidally varying axial load. Subsequently the extracted ATF and ADF parameters are used to represent the constitutive equations and obtain the equations of motion for the continuum of a generally multilayered viscoelastic beam, discretized using finite beam elements. These equations of motion are studied for the dynamics of the viscoelastic composite beam.

For an example the dynamics of a cantilevered composite beam made of two concentric layers of Steel and Aluminium is studied, where behaviours of both steel and aluminium are represented by viscoelastic models. It has been observed that proper choice of placement of layers and their thickness ratios help in postponing the first natural frequency, increasing modal damping leading to reduction in vibration response.

2. Constitutive relations and equations of motion

Equations of motion of a beam made of single viscoelastic material have been given by Lesieutre and Mingori (1990) by using ATF approach. For the purpose of writing the equations of motion using the ADF approach, as it is not in the literature, as well as for the sake of completeness, this section is written as an extension of the work by Lesiture and Mingori (1990) and Lesieutre *et al.* (1996).

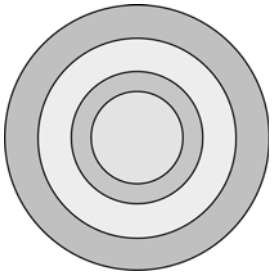

Fig. 1 Beam of multiple viscoelastic layers

2.1 Constitutive relationships

In this section a beam made of several viscoelastic layers has been assumed and correspondingly the equations of motion have been derived by using ATF and ADF approaches. All the layers are assumed to be perfectly bonded and no slip takes place between the layers during bending. Fig. 1 shows the sectional view of a multi-layered beam. The Helmholtz free energy for ATF and ADF approaches of j^{th} layers are given by Eqs. (1a) and (1b) respectively. Corresponding material constitutive relations are given by Eqs. (2a) and (2b).

$$\mathcal{H}_j = \frac{1}{2}(E_j\varepsilon^2 - 2\delta_j\varepsilon\xi_j + \alpha_j\xi_j^2) \tag{1a}$$

$$\mathcal{H}_j = \frac{1}{2}(E_j\varepsilon^2 - 2E_j\varepsilon\varepsilon_j^A + E_j^A\varepsilon_j^{A^2}) \tag{1b}$$

$$\sigma_j = \frac{\partial\mathcal{H}_j}{\partial\varepsilon} = (E_j\varepsilon - \delta_j\xi_j); \quad \mathcal{A}_j = -\frac{\partial\mathcal{H}_j}{\partial\xi_j} = \delta_j\varepsilon - \alpha_j\xi_j \tag{2a}$$

$$\sigma_j = \frac{\partial\mathcal{H}_j}{\partial\varepsilon} = E_j(\varepsilon - \varepsilon_j^A); \quad \sigma_j^A = -\frac{\partial\mathcal{H}_j}{\partial\varepsilon_{jj}^A} = E_j(\varepsilon - c_j\varepsilon_j^A) \tag{2b}$$

where the subscript 'j' stands for the contribution obtained from the j^{th} layer.

In ATF approach E is the elastic modulus, σ is the mechanical stress, ε is the mechanical strain, ξ is the augmenting thermodynamic field (ATF), $\mathcal{A}$ is the affinity, α is a material property relating the changes in $\mathcal{A}$ to ξ and δ is the strength of coupling between the mechanical displacement field and the thermodynamic field.

In the case of ADF approach, E is the elastic modulus, σ is the total stress, ε is the total strain, σ^A is the anelastic stress, ε^A is the anelastic strain, E^A is the anelastic material property and $c = E^A/E$ is a constant.

2.2 Equations of motion of beam made of multiple viscoelastic layers

A uniform, plane, slender beam made of several viscoelastic materials arranged in layers, is considered. When the beam is deformed, it is assumed that a transverse section, originally plane, will remain plane. The stress normal to the transverse plane (parallel to x-axis) is assumed to be the main stress. The x-axis and y-axis are defined to be parallel and perpendicular to the beam axis,

respectively with corresponding displacement components $u(x,y)$ and $v(x,y)$. To this end the following approximations are used.

$$v(x,y) = v(x),\ u(x,y) = -yv'(x) \tag{3}$$

Using the constitutive relations, the equations of motions are obtained as a set of two coupled partial differential equations. The equation of evolution for the mechanical displacement field is developed from the consideration of momentum balance or by assuming zero body force. Assuming the time rate of change of dissipation field is proportional to thermal stress or proportional to its deviation from an equilibrium value, a first order differential equation, i.e., a relaxation equation is obtained

For ATF approach

$$\dot{\xi}_j = S\mathcal{A}_j = -B_j(\xi_j - \bar{\xi}_j) \tag{4a}$$

and for ADF approach

$$\dot{\varepsilon}_j^A = S\sigma_j^A = -b_j(\varepsilon_j^A - \bar{\varepsilon}_j^A) \tag{4b}$$

In the preceding equation B_j or b_j is the inverse of relaxation time for the j^{th} layer, S is a constant of proportionality, and $\bar{\xi}_j, \bar{\varepsilon}_j^A$ denote respectively the values of ξ_j and ε_j at equilibrium where $\mathcal{A}_j = \sigma_j^A = 0$. Putting $\mathcal{A}_j = \sigma_j^A = 0$ in Eqs. (2a) and (2b), the values of $\bar{\xi}_j, \bar{\varepsilon}_j^A$ are obtained as $\bar{\xi}_j = \dfrac{\delta_j}{\alpha_j}\varepsilon$ and $\bar{\varepsilon}_j^A = \dfrac{1}{c_j}\varepsilon$.

The partial differential equation governing the motion of an Euler-Bernoulli beam with no distribution of external load is given by

$$\rho A\ddot{v} = \frac{\partial^2}{\partial x^2}\int_A \sigma y dA \tag{5}$$

where, ρ is the density of the material, A is the cross-sectional area, σ is the stress in a fibre of infinitesimal cross-section at a distance y from the neutral axis of the section. The symbols $(\cdot)$ and $(')$ stand for single partial differentiation with respect to time, $\partial/\partial t$ and space, $\partial/\partial x$ respectively.

Substituting the expression of σ from Eqs. (2) into Eq. (5), putting $\bar{\xi}_j = \dfrac{\delta_j}{\alpha_j}\varepsilon$ and $\bar{\varepsilon}_j^A = \dfrac{1}{c_j}\varepsilon$ in Eq. (4) and using $\varepsilon = \partial u/\partial x = -yv''(x)$, the equations of motion of the beam are obtained by performing the integration over the cross-sectional area and are given as:

For ATF approach as

$$\rho A\ddot{v} + \sum_{j=1}^{N} E_j I_j v'''' = -\sum_{j=1}^{N} \delta_j \int_A \xi_j'' y dA \tag{6a}$$

$$\int_A [\dot{\xi}_j + B_j \xi_j] y dA = -I\left(\frac{B_j \delta_j}{\alpha_j}\right) v'' \tag{6b}$$

and for ADF approach as

$$\rho A\ddot{v} + \sum_{j=1}^{N} E_j I_j v'''' = -\sum_{j=1}^{N} E_j \int_A \varepsilon_j^{A\prime\prime} y dA \tag{7a}$$

$$\int_A [\dot{\varepsilon}_j^A + b_j \varepsilon_j^A] y dA = -I\left(\frac{b_j}{c_j}\right) v'' \tag{7b}$$

where, 'I' is the area moment of inertia $\left(I = \int_A y^2 dA\right)$,

Assuming $\xi_j(x,y,t)$ and $\varepsilon_j^A(x,y,t)$ to vary linearly with the distance of the fibre from the neutral axis, 'y', i.e., $\xi_j(x,y,t) = y f_j(x,t)$ and $\varepsilon_j^A(x,y,t) = y f_j(x,t)$. Eqs. (6b) and and (7b) are rewritten as

$$\int_A \xi_j'' y dA = I f_j'' \tag{8a}$$

$$\int_A \varepsilon_j^{A\prime\prime} y dA = I f_j'' \tag{8b}$$

In the preceding equations, 'f_j', stands for dissipation field for the j^{th} layer due to bending.
Combining Eqs. (6) to (8), the equations of motion for the viscoelastic beam are written
For ATF approach as

$$\rho A\ddot{v} + \sum_{j=1}^{N} E_j I_j v'''' + \sum_{j=1}^{N} \delta_j I_j f_j'' = 0 \tag{9a}$$

$$\dot{f}_j + B_j f_j + \frac{B_j \delta_j}{\alpha_j} v'' = 0 \tag{9b}$$

and for ADF approach as

$$\rho A\ddot{v} + \sum_{j=1}^{N} E_j I_j v'''' + \sum_{j=1}^{N} E_j I_j f_j'' = 0 \tag{10a}$$

$$\dot{f}_j + b_j f_j + \frac{b_j}{c_j} v'' = 0 \tag{10b}$$

2.3 Finite element formulation

For the FE formulation of the spatial continuum, the time varying mechanical displacement $v(x,t)$ and the dissipation coordinate $f(x,t)$ are approximated by $v(x,t) = \phi(x)^T q(t)$ and $f(x,t) = \theta(x)^T p(t)$, where, $\phi(x)$ is the Hermite shape function and $\theta(x)$ is the Lagrange shape function. Galerkin's method is employed to the differential equations to derive the finite element form (Lesieutre and Mingori 1990). Fig. 2 illustrates a beam element and the nodal variables for the two dependent fields.

After FE formulation the ATF and ADF approaches yield the following differential equations

$$([M_T] + [M_R])\{\ddot{q}\} + [K_B]\{q\} = -[J]\{p\} \tag{11a}$$

$$[C]\{\dot{p}\} + [H]\{p\} = -[F]\{q\} \tag{11b}$$

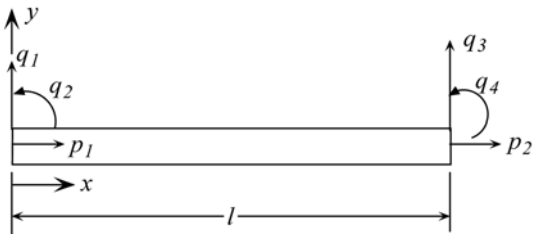

Fig. 2 A damped beam bending element

Where, $M_T = \int_0^l \rho A \phi \phi^T dx$, $M_R = \int_0^l \rho I \phi' \phi'^T dx$ are the mass matrix in translation and the rotary inertia matrix respectively. The rotary inertia matrix has been included to incorporate the effect of the rotation of the cross section of the beam due to bending.

The bending stiffness matrix is given as, $[K_B] = \sum_{j=1}^{N} E_j I_j \int_0^l \phi'' \phi''^T dx$

The other matrices are

$$[J] = [[J_1]_{(4\times 2)} \; [J_2]_{(4\times 2)} \; \cdots \; [J_j]_{(4\times 2)} \; \cdots \; [J_N]_{(4\times 2)}]$$

$$[C] = \begin{bmatrix} [C_1]_{(2\times 2)} & & & & \\ & [C_2]_{(2\times 2)} & & 0 & \\ & & \ddots & & \\ & & & [C_j]_{(2\times 2)} & \\ & 0 & & & \ddots \\ & & & & [C_N]_{(2\times 2)} \end{bmatrix}, \quad [F] = \begin{bmatrix} [F_1]_{(2\times 4)} \\ [F_2]_{(2\times 4)} \\ \vdots \\ [F_j]_{(2\times 4)} \\ \vdots \\ [F_N]_{(2\times 4)} \end{bmatrix}$$

$$[H] = \begin{bmatrix} [H_1]_{(2\times 2)} & & & & \\ & [H_2]_{(2\times 2)} & & 0 & \\ & & \ddots & & \\ & & & [H_j]_{(2\times 2)} & \\ & 0 & & & \ddots \\ & & & & [H_N]_{(2\times 2)} \end{bmatrix}, \quad [p] = \begin{bmatrix} \{p_1\}_{(2\times 1)} \\ \{p_2\}_{(2\times 1)} \\ \vdots \\ \{p_j\}_{(2\times 1)} \\ \vdots \\ \{p_N\}_{(2\times 1)} \end{bmatrix}$$

where, $J_j = \int_0^l \delta_j I_j \phi'' \theta^T dx$, $C_j = \int_0^l \theta \theta^T dx$, $H_j = \int_0^l B_j \theta \theta^T dx$, $F_j = \int_0^l \left(\frac{B_j \delta_j}{\alpha_j}\right) \theta \phi''^T dx$ for ATF approach and

$J_j = \int_0^l E_j I_j \phi'' \theta^T dx$, $C_j = \int_0^l \theta \theta^T dx$, $H_j = \int_0^l b_j \theta \theta^T dx$, $F_j = \int_0^l \left(\frac{b_j}{c_j}\right) \theta \phi''^T dx$ for ADF approach, with 'j' varying from 1 to N, the number of layers used in the model.

Eqs. (11a) and (11b) may be further combined and rewritten as-

$$[\mathcal{A}]\{\dot{X}\} + [\mathcal{B}]\{X\} = \{\mathcal{P}\} \tag{12}$$

where $[\mathcal{A}] = \begin{bmatrix} [M_T]+[M_R] & [0] & [0] \\ [0] & [I] & [0] \\ [0] & [0] & [C] \end{bmatrix}$, $[\mathcal{B}] = \begin{bmatrix} [0] & [K_B] & [J] \\ -[I] & [0] & [0] \\ [0] & [F] & [H] \end{bmatrix}$, $\{X\} = \begin{Bmatrix} \{\dot{q}\} \\ \{q\} \\ \{p\} \end{Bmatrix}$, $\{\mathcal{P}\} = \begin{Bmatrix} \{P\} \\ \{0\} \\ \{0\} \end{Bmatrix}$.

2.4 Modal damping ratio

To obtain the modal damping ratio for multiple viscoelastic layered beam, the complex modulus is derived first. Following Lesieutre (1989) the complex modulus of viscoelastic beam having several layers is obtained by applying Fourier analysis to the equations of motion (Eq. (9) and Eq. (10)). So letting $v = V\mathrm{e}^{\mathrm{i}(\omega t + \mathrm{k}x)}$ and $f_j = Z_j\mathrm{e}^{\mathrm{i}(\omega t + \mathrm{k}x)}$ (where 'ω' is the temporal frequency and 'k' is the spatial frequency or wave number), and substituting these in the Eq. (9a) and Eq. (9b) using ATF approach yields.

$$-\rho\omega^2 V + \frac{1}{A}\sum_{j=1}^{N} E_j I_j \mathrm{k}^4 V - \frac{1}{A}\sum_{j=1}^{N} \delta_j I_j \mathrm{k}^2 Z_j = 0 \tag{13a}$$

$$i\omega Z_j + B_j Z_j - \left(\frac{B_j \delta_j}{\alpha_j}\right) i\mathrm{k}^2 V = 0 \tag{13b}$$

Substituting Z from Eq. (13b) to Eq. (13a) yields

$$-\rho\omega^2 V + \frac{1}{A}\sum_{j=1}^{N} E_j I_j \mathrm{k}^4 V - \frac{1}{A}\sum_{j=1}^{N} \frac{B_j \delta_j^2 I_j}{\alpha_j} \frac{1}{B_j + i\omega} \mathrm{k}^4 V = 0 \tag{14}$$

After separating the real and imaginary parts of the preceding equation, the complex modulus is found as

$$E^*(\omega) = \frac{1}{A}\sum_{j=1}^{N} E_j I_j \left(1 - \left(\frac{\delta_j^2}{E_j \alpha_j}\right) \frac{1}{1 + \left(\frac{\omega}{B_j}\right)^2}\right) + \frac{i}{A}\sum_{j=1}^{N} E_j I_j \left(\left(\frac{\delta_j^2}{E_j \alpha_j}\right) \frac{\left(\frac{\omega}{B_j}\right)}{1 + \left(\frac{\omega}{B_j}\right)^2}\right) \tag{15a}$$

Following the same method, the complex modulus obtained from the ADF approach is given as

$$E^*(\omega) = \frac{1}{A}\sum_{j=1}^{N} E_j I_j \left(1 - \frac{1}{c_j} \frac{1}{1 + \left(\frac{\omega}{b_j}\right)^2}\right) + \frac{i}{A}\sum_{j=1}^{N} E_j I_j \left(\frac{1}{c_j} \frac{\left(\frac{\omega}{b_j}\right)}{1 + \left(\frac{\omega}{b_j}\right)^2}\right) \tag{15b}$$

The modal damping ratio in the ATF approach is given as

$$\varsigma_{\mathrm{n}} = \frac{1}{2}\frac{\sum_{j=1}^{N} E_j I_j \left(\left(\frac{\delta_j^2}{E_j \alpha_j} \right) \frac{\left(\frac{\omega_{\mathrm{n}}}{B_j} \right)}{1 + \left(\frac{\omega_{\mathrm{n}}}{B_j} \right)^2} \right)}{\sum_{j=1}^{N} E_j I_j \left(1 - \left(\frac{\delta_j^2}{E_j \alpha_j} \right) \frac{1}{1 + \left(\frac{\omega_{\mathrm{n}}}{B_j} \right)^2} \right)} \tag{16a}$$

For ADF approach

$$\varsigma_{\mathrm{n}} = \frac{1}{2}\frac{\sum_{j=1}^{N} E_j I_j \left(\frac{1}{c_j} \frac{\left(\frac{\omega_{\mathrm{n}}}{b_j} \right)}{1 + \left(\frac{\omega_{\mathrm{n}}}{b_j} \right)^2} \right)}{\sum_{j=1}^{N} E_j I_j \left(1 - \frac{1}{c_j} \frac{1}{1 + \left(\frac{\omega_{\mathrm{n}}}{b_j} \right)^2} \right)} \tag{16b}$$

where, ω_n is the n^{th} modal frequency of the beam, which can be determined from the eigenvalues of the free vibration equation of Eq. (12).

3. Finding out the viscoelastic parameters

3.1 Model parameters from hysteresis

This section attempts to find out the values of the viscoelastic parameters (B, α, δ) for ATF approach and (b, c) in the ADF approach from the values of storage modulus and loss factors usually given in handbooks. Genetic algorithm has been used for finding out those parameters. Viscoelastic parameters have been found out by minimizing the objective function, constructing the error between the hysteresis obtained by the complex modulus approach and the same in the ATF or ADF approach, at any frequency of excitation. A code in MATLAB (version 7.1) has been written for obtaining the viscoelastic parameters of the material.

As an example, a steel rod (Length 0.75 m and outer diameter 0.05 m) is considered to be acted upon a sinusoidal axial load $(P = 1\ \mathrm{N})$, as shown in the Fig. 3. The material properties of steel (Lazan (1968)) are E = 2.1e11 Pa, η = 1.6e-3 ρ = 7800 kg/m^3. The equations of motion of uniaxial viscoelastic rod using ATF and ADF approaches have been taken from Lesieutre and Mingori (1990) and Lesieutre *et al.* (1996) respectively.

Fig. 4 compares the force displacement plots obtained by using ATF, ADF and complex modulus approaches. Response and energy dissipation for various excitation frequencies have been shown in Fig. 5. Close match in all these plots proves the correctness of the viscoelastic parameters.

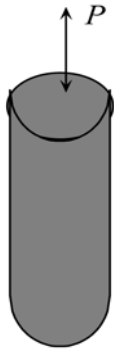

Fig. 3 Schematic diagram of a bar

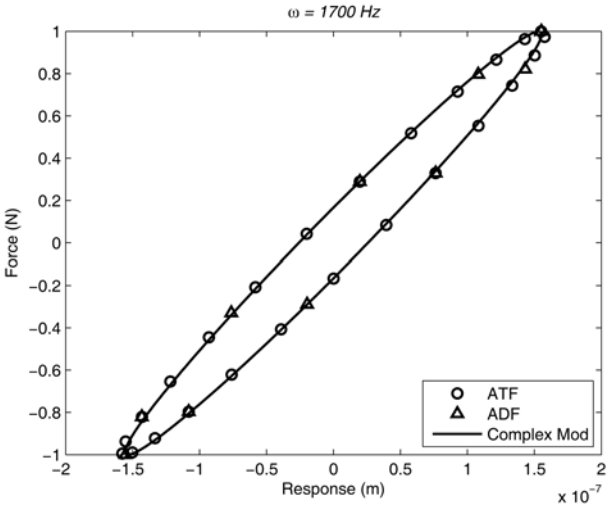

Fig. 4 Hysteresis loop

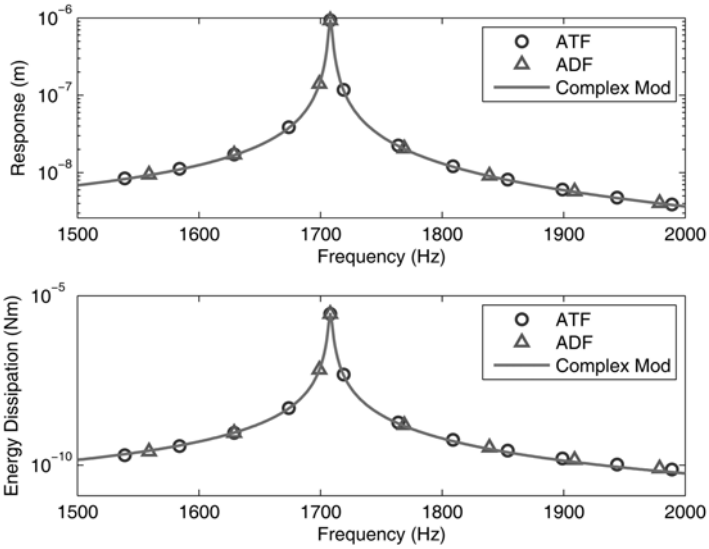

Fig. 5 Response and energy dissipation

Based on the minimization of the error between the hysteresis predicted by the complex modulus approach and the ATF and ADF approaches, values of the viscoelastic parameters are found out. These are B = 1.807e5, α = 1.807e5, δ = 3.186e7 and b = 1.807e5, c = 37.3748.

3.2 ATF parameters from ADF parameters

As a part of this extraction process it was felt necessary to set up relationships among the model parameters in different approaches so that knowing model parameters in one approach enables one to calculate the parameters in another approach. Yet again it may be seen that extracting the ADF parameters is easier and less time consuming than the ATF parameters as number and the range of values of ADF parameters are lesser than those of the ATF parameters. Comparing the expressions of complex modulii for ATF and ADF approaches as given in Eqs. (15a) and (15b), the ATF parameters in terms of the ADF parameters for j^{th} layer are found out as given below.

$$B_j = b_j, \quad \alpha_j = B_j, \quad \delta_j = \sqrt{\frac{E_j b_j}{c_j}}$$

4. Forced response of a beam

The force vector $\{\mathcal{P}\}$ in Eq. (12) is written as $\mathcal{P} = \bar{\mathcal{P}} e^{i\omega t}$. The vector $\{\bar{\mathcal{P}}\}$ contains amplitude of excitation vectors at the excitation nodes.

Substituting a trial solution $\{\mathcal{X}\} = \{\bar{\mathcal{X}}\} e^{i\omega t}$ in Eq. (12) yields

$$\{\bar{\mathcal{X}}\} = [[\mathcal{B}] + i\omega[\mathcal{A}]]^{-1}\{\bar{\mathcal{P}}\} = [\beta(\omega)]\{\bar{\mathcal{P}}\} \tag{17}$$

where $[\beta(\omega)]$ in the preceding equation is the frequency response function (FRF) matrix.

The response amplitude at the n^{th} node is given by $X_n = \max(\text{Real}(\bar{X}_n e^{i\omega t}))$
where, Real( ) stands for the real part of the complex number.

5. Results and discussions

5.1 Response amplitude and modal damping ratio of a viscoelastic beam

A cantilever beam made of steel (Length L = 0.75 m and outer diameter d_0 = 0.05 m) as shown in Fig. 6 is considered. The material properties of steel are E = 200 GPa, η = 1.6e-3 ρ = 7800 kg/m^3 and the viscoelastic parameters of steel using ATF and ADF approach are B = 1.807e5, α = 1.807e5, δ = 3.186e7 and b = 1.807e5, c = 37.3748 as given in section 3. The beam is subjected to harmonic excitation at the tip. The amplitude of transverse load (P) is taken as 1 N.

Table 1 shows the nice agreement of three consecutive modal damping ratios and natural frequencies by using ATF and ADF approaches. The damping ratios have been found out from the complex modulus.

Fig. 7 shows the response amplitude at the tip for different excirarion frequencies. The curve has two peaks which indicate the first and second natural frequencies. The plot shows that the ATF and ADF formulations predict the same response amplitude.

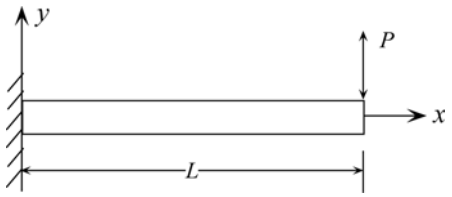

Fig. 6 Schematic diagram of a cantilevered beam

Table 1 Damping ratio and natural frequency for three consecutive modes

Method	Ist mode		2nd mode		3rd mode	
	Damping ratio	Natural frequency (Hz)	Damping ratio	Natural frequency (Hz)	Damping ratio	Natural frequency (Hz)
ATF	3.0397e-5	63.6141	1.8974e-4	397.1491	5.2744e-4	1.1055e+3
ADF	3.0405e-5	63.6139	1.8978e-4	397.1477	5.2757e-4	1.1055e+3

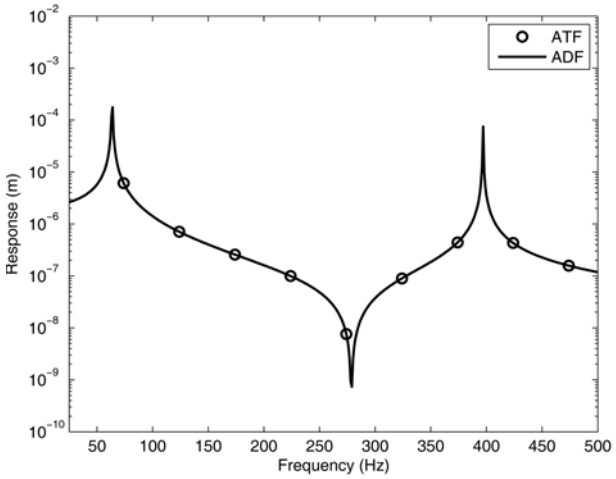

Fig. 7 Beam Response amplitude

5.2 Beams of multiple viscoelastic layers

The equations of motion of beams composed of multiple viscoelastic layers have been discussed in section 2.3. In this section a specific example of a beam using two viscoelastic layers (Fig. 8) has been considered. Fig. 8 shows the beam of two concentric sections of different materials of densities ρ_{i} and ρ_{o}. The radius ratio of the section and equivalent density are defined as

$$\Re = \frac{r_{\mathrm{i}}}{r_{\mathrm{o}}}, \quad \rho = \rho_{\mathrm{i}}\Re^2 + \rho_o(1-\Re^2) \tag{18}$$

If the inner and outer materials are interchanged keeping the masses of the inner and outer material unchanged the radius ratio becomes

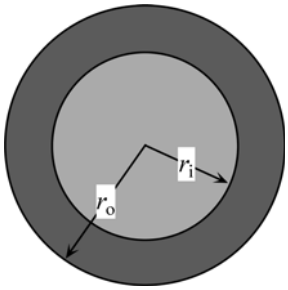

Fig. 8 Beam of two materials

$$\Re' = \sqrt{1 - \Re^2} \tag{19}$$

As $\Re \to 0$ the whole cross section is filled by the outer material of density ρ_o, and $\Re \to 1$ when the cross section is made of the inner material of density of ρ_i.

For an example the same beam as in section 5.1 (Length $L = 0.75$ m and outer diameter $D = 0.05$ m) is considered to have two materials (similar to the one shown in Fig. 8), aluminium and steel, one forming the core and the other the outer layer. Following Lesieutre and Mingori (1990) the material properties of aluminium are taken as $E = 7.13e10$ Pa, $\rho = 2750$ kg/m^3 and the viscoelastic parameters in ATF approach are as $B = 8000$, $\alpha = B$, $\delta = 4.7766e6$. The corresponding properties of steel are taken as $E = 2.1e11$ Pa, $\rho = 7800$ kg/m^3, $B = 1.807e5$, $\alpha = 1.807e5$, $\delta = 3.186e7$, as given in section 3.

5.2.1 Modal damping ratio and change in the First Natural Frequency in bending

Fig. 9 shows the modal damping ratio (ζ) for various radius ratios ($\Re$). The study has been carried out for both placements of aluminium and steel, i.e., steel as core and aluminium forming the outer layer and vice versa. When steel forms the core and aluminium forms the outer layer (Case-I), $\Re$ is defined as $\Re = r_i/r_o = r_{steel}/r_o$. It is seen from the figure that, for this case (as shown by the dotted line) ζ decreases with increasing values of $\Re$ as steel provides lesser damping than aluminium. The solid lines show the corresponding values of ζ, when for the same beam mass aluminium forms the core and steel forms the outer layer (Case-II), and the radius ratio is $\Re' = \sqrt{1 - \Re^2}$ as shown in Eq. (19). For this placement the values of modal damping ratio fall because, firstly aluminium being placed as the core material is not subjected to flexural rate as high as the former situation (Case-I) and secondly the placement of steel on the outer layer enhances modal stiffness as it undergoes higher deformation due to bending in comparison with the earlier situation (Case-I).

Fig. 10 shows the % change in First Natural Frequency (FNF) with respect to the case of an all aluminium beam for various values of $\Re$. The dotted line is for Case-I whereas the solid line represents the results corresponding to Case-II. In consonance with the observation held in explaining Fig. 9 the FNF in Case-II (for which the change is always positive) is found to be more than that for Case-I (for which the change is always negative) always. From the figure it is seen that there exists an optimum value of $\Re$ beyond which the FNF in Case-II starts decreasing. This is due to the fact that the equivalent density increases with $\Re$, as specific gravity of steel is more than that of aluminium. So a critical value of $\Re$ is reached when aluminium forms the core and steel the outer layer. For an example the value of $\Re$ corresponding to the maximum increment of FNF (15%) for Case-II is found to be 0.6 which corresponds to a value of $\Re' = 0.8$. For the dimensions chosen,

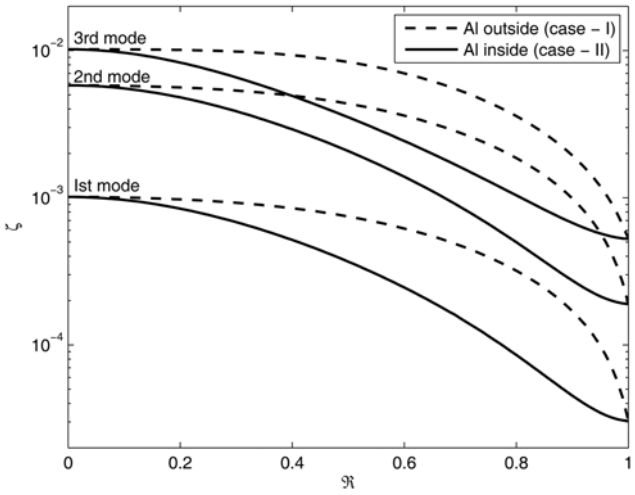

Fig. 9 Modal damping ratio at various radius ratios

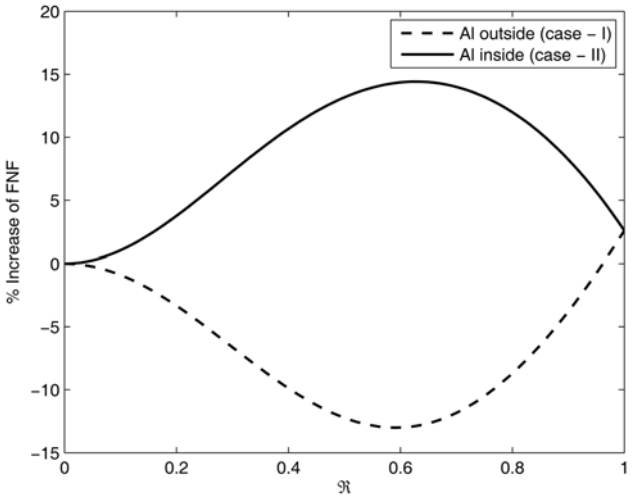

Fig. 10 First natural frequency at various radius ratios

the beam is composed of an aluminium core of diameter 0.04 m with an outside steel layer of thickness 0.005 m. Thus with proper dimension and placement of materials the natural frequencies may be substantially increased. This is the utility of using a composite beam.

5.2.2 Response due to harmonic excitation

The beam is subjected to transverse harmonic excitation of amplitude 1 N at the tip. Fig. 11 shows the response amplitude plotted at several excitation frequencies for different values of $\Re$ as well as different placements (inside and outside) of aluminium and steel. For Case-I the resonance peaks occur earlier as $\Re$ increases; this is in keeping with the findings in Fig. 10 where FNF is seen to fall initially as $\Re$ increases as the mass of the beam increases more than its stiffness as the radius of steel core increases. For Case-II however the peak shifts to the right as $\Re$ increases; this behaviour may similarly be explained from Fig. 10. As the resonance gets postponed, the response

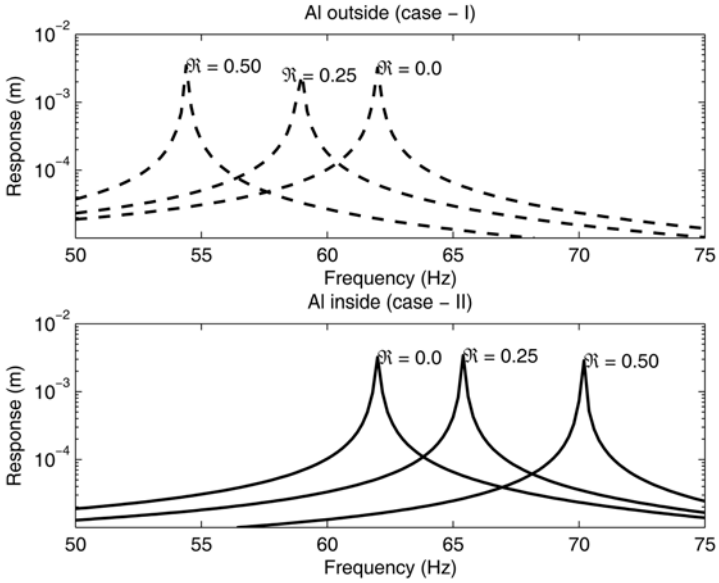

Fig. 11 Response amplitude at various radius ratios

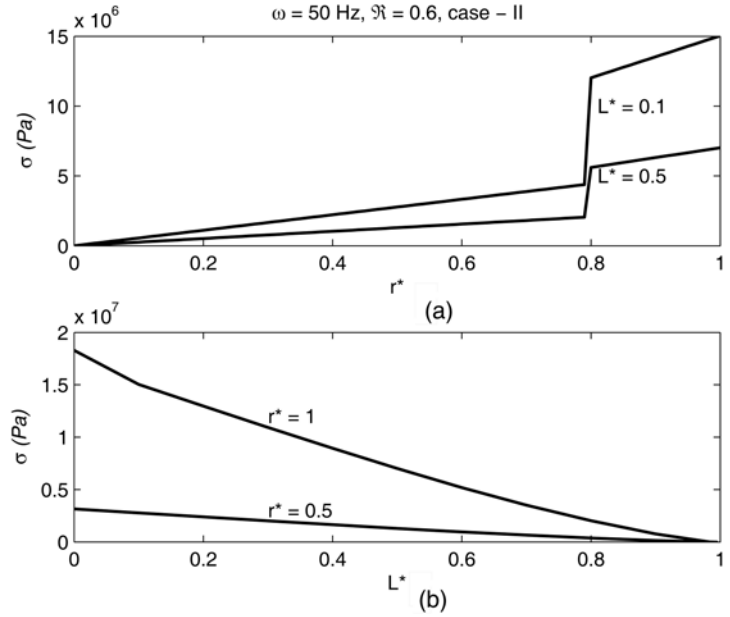

Fig. 12 Mechanical stress at various section

amplitude below the resonant frequency keeps falling as $\Re$ increases. For an example a value of $\Re$ = 0.5 in the present configuration (Length L = 0.75 m and outer diameter D = 0.05 m) will give a core radius of steel = 0.0125 m with an aluminium outer layer of 0.0125 m. A beam same as mass of this beam will be composed of an aluminium core of radius 0.0217 m and a steel outer layer of thickness 0.0033 m corresponding to a value of $\Re'$ = 0.866 as in Case-II.

Fig. 12(a) shows the amplitude of stress distribution of a composite beam with an aluminium core

of diameter 0.04 m and steel layer of thickness 0.005 m ($\Re' = 0.8$) at sections $L^* = 0.1$ and 0.5 where $L^* = l/L$ and $r^* = r/r_o$, 'l' being the distance of the beam section from the root, 'r' being the radial location of any point and $r_o = 0.025$ m is the outer radius of the beam cross-section. It is seen that as the point moves from aluminium domain to the steel domain, the stress increases suddenly as steel has higher modulus of elasticity. Similarly the Fig. 12(b) shows the variation of stress amplitude as the section is shifted along the length of the cantilever from the fixed to the free end. The stress amplitude is seen to fall as expected from root to the tip however the stress magnitude in steel always remains more than that of aluminium.

6. Conclusions

1. The ATF & ADF approach introduce internal variables which are very efficient in modelling frequency dependent viscoelastic material properties in the time domain.
2. It has been noticed that the ADF approach is more convenient to apply than the ATF approach as the number of parameters and their range of values in ADF are less than those in ATF approach.
3. By proper placement of the composite layers and proper selection of thickness ratios, the first natural frequency may be sufficiently postponed leading to reductions in vibration response.

References

Bagley, R.L. and Torvik, P.J. (1983), "Fractional calculus - a different approach to the analysis of viscoelatically damped structures", *AIAA J.*, **21**(5), 741-748.

Bagley, R.L. and Torvik, P.J. (1985), "Fractional calculus in the transient analysis of viscoelatically damped structure", *AIAA J.*, **23**(3), 201-210.

Golla, D.F. and Hughes, P.C. (1985), "Dynamics of viscoelastic structures - a time domain finite element formulation", *J. Appl. Mech.*, ASME, **52**, 897-906.

Lazan, B.J. (1968), *Damping of Materials and Members in Structural Mechanics*, London: Perg-amon Press.

Lesieutre G.A. (1989), "Finite element modeling of frequency-dependent material damping using augmenting thermodynamic fields", PhD thesis, University of California, Los Angeles.

Lesieutre, G.A. (1992), "Finite elements for dynamic modelling of uniaxial rods with frequency-dependent material properties", *Int. J. Solids Struct.*, **29**(12), 1567-1579.

Lesieutre, G.A. and Bianchini, E. (1995), "Time domain modelling of linear viscoelasticity using anelastic displacement fields", *J. Vib. Acoust.*, ASME, **17**(4), 424-430.

Lesieutre, G.A. and Mingori, D.L. (1990), "Finite element modelling of frequency- dependent material damping using augmenting thermodynamic fields", *J. Guidance, Control Dyn.*, AIAA, **13**(6), 1040-1050.

Lesieutre, G.A., Bianchini, E. and Maiani, A. (1996), "Finite element modeling of one-dimensional viscoelastic structures using anelastic displacement fields", *J. Guidance and Control*, **19**(3), 520-527.

McTavish, D.J. and Hughes, P.C. (1992), "Prediction and measurement of modal damping factors for viscoelastic space structures", *AIAA J.*, **30**(5), 1392-1399.

McTavish, D.J. and Hughes, P.C. (1993), "Modeling of linear viscoelastic space structures", *J. Vib. Acoust.*, ASME, **115**(1), 103-110.

Roy, H., Dutt, J.K. and Datta, P.K. (2008), "Dynamics of a viscoelastic rotor shaft using augmenting thermodynamic fields—A finite element approach", *Int. J. Mech. Sci.*, **50**, 845-853.

Notation

A : cross-sectional area of the beam
$\mathcal{A}$: affinity, a thermodynamically conjugate to ξ
b, B : inverse of relaxation time
E : unrelaxed elastic modulus
E^A : anelastic material property
f : ATF or ADF for beam bending, corresponding to ξ or ε^A
$\mathcal{H}$: Helmholtz free energy density function
I : area moment of inertia
l : element length
L : length of the beam
L^* : non-dimensional distance from the root
$\underline{p}$: vector of ADF or ATF displacements
$\overline{\mathcal{P}}$: amplitude of harmonic excitation
q : vector of mechanical displacements
r_i : radius occupied by the inner material
r_o : outer radius of the beam
r^* : non-dimensional distance from the neutral surface
$\mathfrak{R}$: radius ratio, $\mathfrak{R} = r_\mathrm{i}/r_\mathrm{o}$
t : time in sec
u, v : mechanical displacement corresponding to the x and y axis respectively
α : material property relating changes in $\mathcal{A}$ to those in ξ
β : frequency response function (FRF) matrix
δ : strength of coupling between the mechanical displacement field and the thermodynamic field
ε : mechanical strain
ε^A : anelastic strain
ϕ : Hermite shape function
θ : Lagrange shape function
ρ : equivalent density of the composite material i.e., layered beam
σ : mechanical stress
σ^A : anelastic stress
ς : modal damping ratio
ω : excitation frequency
ω_n : modal frequency
ξ : ATF displacement